World Academy of Science, Engineering and Technology
International Journal of Mechanical and Mechatronics Engineering
Vol:10, No:9, 2016

Numerical Investigation of the Performance of a Vorsyl Separator Using a Euler-Lagrange Approach

Guozhen Li, Philip Hall, Nick Miles, Tao Wu, Jie Dong

***Abstract*—**This paper presents a Euler-Lagrange model of the water-particles multiphase flows in a Vorsyl separator where particles with different densities are separated. A series of particles with their densities ranging from 760 kg/m^3 to 1380 kg/m^3 were fed into the Vorsyl separator with water by means of tangential inlet. The simulation showed that the feed materials acquired centrifugal force which allows most portion of the particles with a density less than water to move to the center of the separator, enter the vortex finder and leave the separator through the bottom outlet. While the particles heavier than water move to the wall, reach the throat area and leave the separator through the side outlet. The particles were thus separated and particles collected at the bottom outlet are pure and clean. The influence of particle density on separation efficiency was investigated which demonstrated a positive correlation of the separation efficiency with increasing density difference between medium liquid and the particle. In addition, the influence of the split ratio on the performance was studied which showed that the separation efficiency of the Vorsyl separator can be improved by the increase of split ratio. The simulation also suggested that the Vorsyl separator may not function when the feeding velocity is smaller than a certain critical feeding in velocity. In addition, an increasing feeding velocity gives rise to increased pressure drop, however does not necessarily increase the separation efficiency.

***Keywords*—**Vorsyl separator, separation efficiency, CFD, split ratio.

I. Introduction

PLASTICS, due to their low cost, versatility, ease of manufacture, and imperviousness to water, have become increasingly indispensable materials used in various products displacing many traditional materials, such as wood, stone, metal, glass, and ceramic, etc. The increase in plastic consumption results in the increase in solid wastes as eventually all plastic products become waste and need to be taken care of. Plastic wastes cause significant environmental problems. Discharging waste plastics directly would pollute the environment. Landfilling them occupies a great number of lands since plastics need a very long time to be degraded [1]. Burning them would produce toxic gases known as dioxin and hydrogen chloride. Therefore, the separation and recycling of waste plastics are of great significance [2]. Various separation methods for waste plastics have been developed by previous researchers which include manual separation, gravity separation, flotation separation, solvent separation, hydrocyclonic separation etc. [1]-[3].

Yuan et al. carried out study on the hydrocyclonic separation of waste plastics with different density. Based on the difference in density, PET and PVC particles were separated with help of the centrifugal sedimentation and shearing dispersion in a hydrocyclone. The relationship between the separating efficiency and pressure drop and split ratio has been investigated [2]. A cyclone separator is able to separate plastics (e.g. PP and PVC) with one's density higher than water and the other's lighter than water with the density difference between two types of plastics being greater than 500 kg/m^3 [2].

The principle of separation in a Vorsyl separator is exactly similar to that of the cyclone separator. The Vorsyl separator, developed by the National Coal Board UK, uses the centrifugal force for the separation of light coal from the heavy refuse in a dense medium. The Vorsyl separator is different from the dense medium cyclone in that firstly the zero axial velocity or dead zone present in the dense medium cyclone is not found in the Vorsyl separator and secondly there exists a strong recirculation of near-gravity material in the Vorsyl separator [4]. Banerjee et al. reported the superiority of Vorsyl separator over dense medium cyclone for treating very high near-gravity material at plant scale [5].

From published research, the application of Vorsyl separator is limited to the separation of coal. Its application in the recycling of plastics waste is still lack of attention. This paper attempts to numerically investigate the potential of Vorsyl separator on separation of plastic particles with one's density higher than water and the other's lighter than water. The trajectory of particles was examined; the effects of density difference between particle and water, the split ratio and the feeding velocity on the separation performance of the Vorsyl separator were analyzed. A good separation effect was predicted suggesting that the Vorsyl separator may serve as a promising alterative device for recycling plastic wastes.

II. Vorsyl Separator

Vorsyl separators with various diameters have been tested experimentally by previous researchers. For instance, Abbott et al. investigated a Vorsyl separator with a diameter of 610 mm and later developed a Vorsyl separator of 720 mm [4]. Banerjee et al. conducted trials on 400 and 600-mm Vorsyl separators made of mild steel, at the captive washeries of the Tata Iron and Steel [5]. Rao et al. reported the performance of a 76 mm Vorsyl separator in a laboratory scale as an alternate for

Guozhen Li is with the University of Nottingham Ningbo China, 199 Taikang East Road, Ningbo, 315100, China (e-mail: Guozhen.LI@nottingham.edu.cn).

Philip Hall is with the University of Nottingham Ningbo China, 199 Taikang East Road, Ningbo, 315100, China (corresponding author: phone: +86(0)574 8818 0018; e-mail: Philip.Hall @nottingham.edu.cn).

Nick Miles, Tao Wu, and Jie Dong are with the University of Nottingham Ningbo China, 199 Taikang East Road, Ningbo, 315100, China.

a dense medium cyclone [4]. In this numerical study, a 105mm Vorsyl separator were investigated as an immediate PMMA model is available in the lab and this size is suitable for a laboratory scale test to be followed.

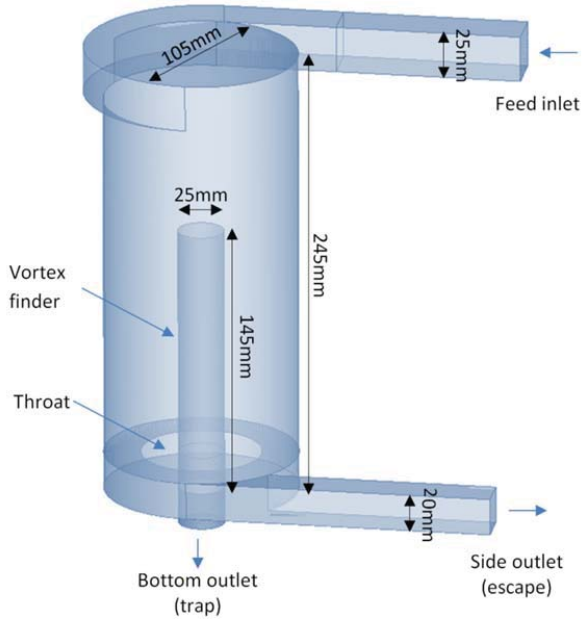

Fig. 1 Schematic diagram of Vorsyl separator

The geometry of the 105 mm Vorsyl separator used in the CFD model is demonstrated in Fig. 1. The Vorsyl separator is arranged vertically and the particles with different densities are fed tangentially into the separator with water from the feed inlet. A vortex finder with a length of 145 mm is fixed from the base of the separator, which is surrounded by an annular space called the throat. Particles with a density less than the separation density move to the center of the separator and leaves through the vortex finder (from bottom outlet). The near gravity particles and those have larger densities than the separation density move to the wall and reach the throat area and leave from the side outlet.

III. Numerical Method and Models

This section introduces the numerical method and the models used for the modelling.

A. Flow Domain

Configuration of the computational domain for use with ANSYS Fluent is shown in Fig. 1. It consists of a tangential feed inlet for the injection of water and particles into the separator, a vortex finder, a throat and two outlets at the bottom and side respectively. The dimension of each component is referred to Fig. 1.

B. Meshing

Before the governing equations can be numerically solved, the flow domain including the surface of all the boundaries need to be discretized into a finite number of elements known as control volumes by the regular or irregular arrangement of nodes, namely the mesh. Flow parameters are resolved around these nodes, so that the fluid flow can be described mathematically by specifying its velocity at all points in space and time.

Unstructured tetrahedral girds were used in the spatial discretization of the flow domain. The use of tetrahedral mesh significantly reduces the amount of time spent generating meshes as it is created by automatic mesh generation algorithms. The unstructured mesh can handle more complex geometries due to its flexibility. In addition, an unstructured mesh made up of triangular or tetrahedral cells created for complex geometries often has far fewer cells than the equivalent structured mesh consisting hexahedral cells.

The maximum mesh size is 3 mm which is fine enough to ensure the convergence of the solution. A quick mesh independence test was carried out so that the errors associated with the size of mesh were minimized.

The bottom view of the separator and the surface meshes of the feed inlet, bottom outlet and side outlet are shown in Fig. 2.

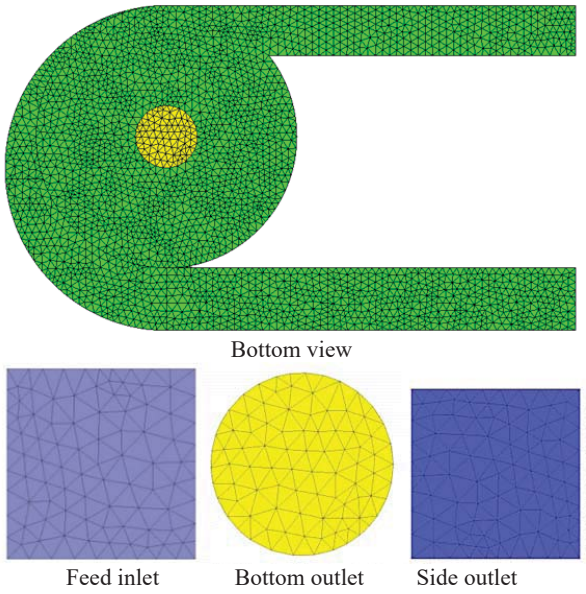

Fig. 2 Schematic diagram of Vorsyl separator

C. Numerical Model Description

Currently, three approaches can be used for the numerical calculation of multiphase flows: The Euler-Lagrange approach, the Euler-Euler approach, and the Dense Discrete Phase Model which is a hybrid Euler-Euler and Euler-Lagrange approach [6]. The Euler-Lagrange approach is a method to look at the fluid motion where the viewer follows a discrete fluid parcel as it travels through space and time. Plotting the position of a discrete parcel through time gives the pathline of the parcel. This can be seen as sitting in a boat and traveling down a river. Whist the Euler-Euler method is an approach of seeing the fluid motion that focuses on specific locations in the space over which the fluid drifts with time. This can be imagined by staying on the bank of a river and looking the water drift the fixed location. In this study, the Euler-Lagrange approach was adopted where the fluid phase

(water) is treated as a continuum by solving the time-averaged Navier-Stokes equations, while the dispersed phase (particles) is solved using a Discrete Phase Model by tracking a large number of particles through the calculated water field. The dispersed phase can exchange mass, momentum, and energy with the liquid phase. This Euler-Lagrange approach can be done with or without including particle-particle interactions depending on the amount of complexity and the amount of computational expense the user wants to spend. In this paper, as a preliminary study, the particle-particle interactions and the influence of particles on the fluid phase were neglected.

In ANSYS Fluent, the trajectory of a discrete phase particle is predicted by integrating the force balance on the particle (written in a Lagrangian reference frame). This force balance equals the particle inertia with the forces acting on the particle, which can be written in Cartesian coordinates as [6]:

$$\frac{du_p}{dt} = F_D\left(\vec{u} - \vec{u}_p\right) + \frac{\vec{g}(\rho_p - \rho)}{\rho_p} + \vec{F} \quad (1)$$

where $\vec{F}$ is an additional acceleration term, $F_D\left(\vec{u} - \overrightarrow{u_p}\right)$ is the drag force per unit particle mass and

$$F_D = \frac{18\mu}{\rho_p d_p^2}\frac{C_D Re}{24} \quad (2)$$

Here $\vec{u}_p$ is the particle velocity, $\vec{u}$ is the fluid phase velocity, μ is the molecular viscosity of the fluid, ρ_p is the density of the particle, ρ is the fluid density, and d_p is the particle diameter. Re is the relative Reynolds number, defined as

$$Re \equiv \frac{\rho d_p |\vec{u}_p - \vec{u}|}{\mu} \quad (3)$$

As for the continuous phase of water, its flow field was predicted by solving the time-averaged Navier-Stokes equations (RANS approach). As the flow within the Vorsyl separator is swirling due to the tangential injection, and in such turbulent flows viscosity is typically anisotropic, therefore the most reliable turbulence model Reynolds Stress Model (RSM) was chosen [7], [8]. The Reynolds Stress Model closes the RANS equations by solving transport equations for the Reynolds stresses, along with an equation for the dissipation rate. Therefore, it required seven additional transport equations for 3D flows. As the Reynolds Stress Model includes the influences of swirl, rotation, streamline curvature, and rapid changes in strain rate in a more rigorous manner than the one-equation and two-equation models, it is of greater potential to give more accurate predictions for complex flows [6]. The transport equations for the transport of the Reynolds Stresses are referred to [8] and [9].

A two-layer-based, non-equilibrium wall function was employed in the near-wall region in order to resolve the velocity gradient and flow behavior in the near-wall region. The non-equilibrium wall function is superior to standard wall function as it accounts for the effects of pressure gradients in the wall area.

D. Simulation Set-Up

Materials

Simulations of the continuous phase were carried out with water, and the flow was assumed to be steady and isothermal. The water density and viscosity were specified as 998.2 kgm^{-3} and 1.003×10^{-3} $kgm^{-1}s^{-1}$.

The particles were then injected into the separator using the Discrete Phase Models by defining the initial position, velocity, and size of individual particles. These initial conditions, along with the inputs defining the physical properties of the discrete phase, are used to initiate trajectory and mass transfer calculations. The trajectory and mass transfer calculations are based on the force balance on the particle and on the mass transfer from the particle, using the local continuous phase conditions as the particle moves through the flow [6]. Particles with various densities were feed into the separator to see the relation between density and separation efficiency. The detailed information of the particles used in the simulation is listed in Table I.

TABLE I
PROPERTIES OF PARTICLES USED IN SIMULATION

Name	Density (kg/m^3)	Diameter (mm)
Particle-0.76	760	3
Particle-0.86	860	3
Particle-0.92	920	3
Particle-0.94	940	3
Particle-0.96	960	3
Particle-1.08	1080	3
Particle-1.18	1180	3
Particle-1.28	1280	3
Particle-1.38	1380	3

Boundary Conditions

At the feed inlet, a velocity inlet boundary condition was used. The turbulence was specified in terms of intensity and hydraulic diameter at both the inlet and outlet. Initially, the simulations were carried out with inlet velocities being 3.6m/s. particles were fed into the separator with the same velocity as water.

Outflow boundary condition was imposed at the bottom and side outlet of the Vorsyl separator respectively. This boundary condition allows specifying the flow rate weighting at each outlet. Initially the flow rate weighting was set to be 0.5 for each outlet which means that half of the liquid flow out through bottom outlet while another half through the side outlet. A 'trap' discrete phase boundary condition was assigned to the bottom outlet whilst a 'escape' discrete phase boundary condition was assigned to the side outlet. The trap boundary condition terminates the trajectory calculations and records the fate of the particle as "trapped", while an escape boundary condition reports the particle as having "escaped". To track the motion of the particles, the spherical drag law, the virtual mass force and the pressure gradient force were included.

The pipe walls were specified as being stationary and no slip walls to match the simulation conditions. The

Non-Equilibrium wall functions were applied in the near wall region.

Solver

Pressure-based Segregated Solver was chosen for the steady state simulation. Absolute velocity formulation was used.

Solution Methods

The SIMPLE discretization technique was applied for the pressure-velocity coupling. A second order upwind scheme was employed for viscous terms.

Convergence Criterion

The convergence criterion used for all cases was that the scaled residuals of x, y, z velocities, k, and ε, and Reynolds stresses have decreased by three orders of magnitude. The mass flow rate at the outlet was also monitored and the solution was deemed to have reached a steady state when this parameter achieved a constant value over a large number of iterations.

IV. Results and Discussions

A. Trajectory of Particles in the Vorsyl Separator

The particles were tracked after being fed into the Vorsyl separator with water. Taking the trajectory of the particle-1.38, particle-0.96 and particle-0.76 for instance, the feed materials entered the Vorsyl separator tangentially and acquired centrifugal force ($F = m\omega^2 r$). The particle-0.76 which has a clearly less density than water tends to move to the centre of the separator and leave through the vortex finder. The particle-1.38 which is heavier than water moves to the wall and reaches the throat area and leave the separator through the side outlet [5]. For particle-0.96 particles which have a density that is only slightly less than water, its trajectory shows that some portion of them reach the vortex finder and leave the separator through bottom outlet while others through side outlet.

To test the separation performance of the separator, it is set that if a particle reaches the bottom outlet, it is seen as 'trapped'; whilst if a particle reaches the side outlet, it is regarded 'escaped'. Taking the separation of particle-1.38 and particle-0.96 for instance, for each type of particle (1.38 and 0.96), 167 items were fed into the separator with water and tracked. It was found that all the 167 particle-1.38 particles were 'escaped' at the side outlet. While only 49 particle-0.96 particles were 'escaped' at the side outlet, leaving 118 particle-0.96 particles to be 'trapped' at the bottom outlet. Therefore, the separation efficiency for particle-0.96 is 70.6%. However, when particle-0.76 was fed into the separator with particle-1.38, all the 167 particle-0.76 particles were trapped at the bottom outlet therefore the separation efficiency for particle-0.76 is 100%.

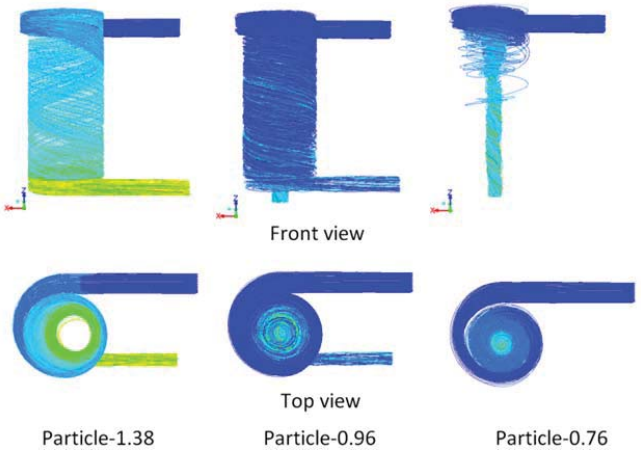

Fig. 3 Trajectory of particles with different densities in the Vorsyl separator

B. Influence of Density on Separation Performance

As shown in Table II, when the density of Particle-1.38 was decrease to Particle-1.28, Particle-1.18 and Particle-1.08 respectively, same separation efficiency is retained as all the particles (heavier than water) leave the Vorsyl separator through side outlet. However, when the density of Particle-0.96 was reduced to Particle-0.94, Particle-0.92, Particle-0.86 and Particle-0.76, the separation efficiency increased to 84.4%, 91%, 97% and 100% respectively. Fig. 4 demonstrates that, for the particles lighter than water, the separation efficiency increases with increasing density difference between the particle and water, and a density difference of 240 kg/m^3 ensures complete separation of the lighter particles (than water) from heaver particles (than water). This density difference of 240 kg/m^3 is smaller than the 500 kg/m^3 required in the cyclone separator [2]. Fig. 4 indicates a positive correlation of the separation efficiency with the density difference between medium liquid and the particle.

TABLE II
Separation of Particles with Different Densities

Name	Escaped at side outlet	Trapped at bottom outlet
Particle-1.38	167 (100%)	0 (0%)
Particle-1.28	167 (100%)	0 (0%)
Particle-1.18	167 (100%)	0 (0%)
Particle-1.08	167 (100%)	0 (0%)
Particle-0.96	49 (39.4%)	118 (70.6%)
Particle-0.94	26 (15.6%)	141 (84.4%)
Particle-0.92	15 (9%)	152 (91%)
Particle-0.86	5 (3%)	162 (97%)
Particle-0.76	0 (0%)	167 (100%)

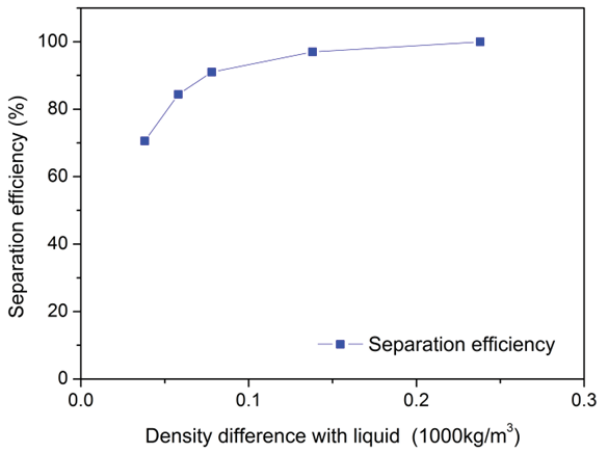

Fig. 4 Correlation of separation efficiency with density difference between particle and water

C. Influence of Split Ratio on Separation Efficiency

The split ratio is defined as the ratio of bottom outlet flow rate to the total flow rate at the feed inlet [2]. Initially the split ratio is 0.5 was used meaning that half of the liquid flow out through bottom outlet while another half through the side outlet. In a real practice, the split ratio can be varied by adjusting a valve near the bottom outlet. A number of cases were run with different split ratio and different particle densities. The simulation showed that split ratio has no obvious influence on the behavior of particles that is heavier than water as they all escape through the side outlet. However, the split ratio does have an influence on the behavior of particles that are lighter than water. Tables III-VII showed that the separation efficiency increases with increasing split ratio.

The effect of split ratio on the separation of particles with different densities is more clearly shown in Fig. 5. It depicts that the positive effect of split ratio is more remarkable on the separation of particles that have a less density difference with water. This suggests that, for the separation of particles that have a density close to the medium liquid, increasing the split ratio may serve as an alternative to make the separation or recycling of such particles possible.

TABLE III
SEPARATION OF PARTICLES UNDER THE SPLIT RATIO OF 0.3

Split ratio 0.3	Escaped at side outlet (0.7 flow rate weighting)	Trapped at bottom outlet (0.3 flow rate weighting)
Particle-0.96	135	32 (19%)
Particle-0.94	72	95 (57%)
Particle-0.92	37	130 (78%)
Particle-0.86	24	143 (85.6%)
Particle-0.76	0	167 (100%)

TABLE IV
SEPARATION OF PARTICLES UNDER THE SPLIT RATIO OF 0.4

Split ratio 0.4	Escaped at side outlet (0.6 flow rate weighting)	Trapped at bottom outlet (0.4 flow rate weighting)
Particle-0.96	81	86 (51.5%)
Particle-0.94	36	131 (78%)
Particle-0.92	22	145 (87%)
Particle-0.86	18	149 (89%)
Particle-0.76	0	167 (100%)

TABLE V
SEPARATION OF PARTICLES UNDER THE SPLIT RATIO OF 0.5

Split ratio 0.5	Escaped at side outlet (0.5 flow rate weighting)	Trapped at bottom outlet (0.5 flow rate weighting)
Particle-0.96	49	118 (70.6%)
Particle-0.94	26	141 (84.4%)
Particle-0.92	15	152 (91%)
Particle-0.86	5	162 (97%)
Particle-0.76	0	167 (100%)

TABLE VI
SEPARATION OF PARTICLES UNDER THE SPLIT RATIO OF 0.6

Split ratio 0.6	Escaped at side outlet (0.4 flow rate weighting)	Trapped at bottom outlet (0.6 flow rate weighting)
Particle-0.96	42	125 (75%)
Particle-0.94	20	147 (88%)
Particle-0.92	8	159 (95%)
Particle-0.86	1	166 (99%)
Particle-0.76	0	167 (100%)

TABLE VII
SEPARATION OF PARTICLES UNDER THE SPLIT RATIO OF 0.7

Split ratio 0.7	Escaped at side outlet (0.3 flow rate weighting)	Trapped at bottom outlet (0.7 flow rate weighting)
Particle-0.96	34	133 (80%)
Particle-0.94	16	151 (90%)
Particle-0.92	13	154 (92%)
Particle-0.86	0	167 (100%)
Particle-0.76	0	167 (100%)

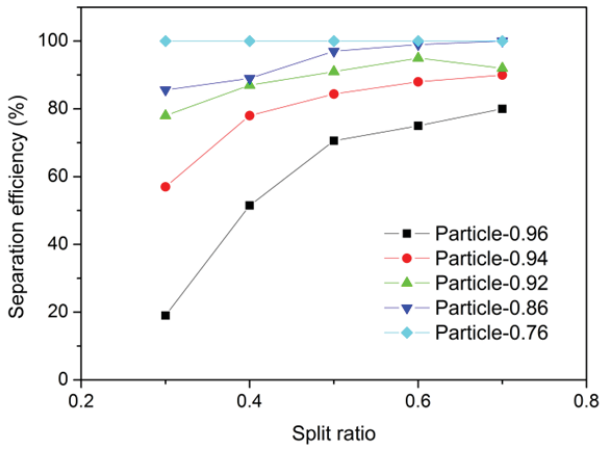

Fig. 5 Correlation of separation efficiency with split ratio

D. Influence of Infeed Velocity on Separation Efficiency

In order to examine the influence of feeding velocity of the water and particles on the separation efficiency, another 11 cases were run covering the inlet velocity of 0.2 m/s, 0.6 m/s, 1 m/s, 1.6 m/s, 2.6 m/s, 4.6 m/s, 5.6 m/s, 6.6 m/s, 7.6 m/s, 8.6 m/s and 9.6 m/s. A split ratio of 0.5 was set in both the bottom and right outlet for all cases.

It was found that, generally, under the conditions simulated, all the particles heavier than the water will eventually reach the side outlet and leave the separator. However, for the particles lighter than water, when the feeding velocity is too low (between 0 m/s and 1.6 m/s), some particles may not be able to leave the separator as they can either reach the bottom nor the side outlet resulting in low separation efficiency. The

separations under these conditions are shown in Tables VIII-X. This may suggest that the separator is not workable below a certain critical feeding velocity.

TABLE VIII
SEPARATION OF PARTICLES UNDER THE INLET VELOCITY OF 0.2 M/S

Inlet velocity: 0.2 m/s	Escaped at side outlet	Trapped at bottom outlet
Particle-0.96	0	0(0%)
Particle-0.94	0	0 (0%)
Particle-0.92	0	0 (0%)
Particle-0.86	0	0 (0%)
Particle-0.76	0	0 (0%)

TABLE IX
SEPARATION OF PARTICLES UNDER THE INLET VELOCITY OF 0.6 M/S

Inlet velocity: 0.6 m/s	Escaped at side outlet	Trapped at bottom outlet
Particle-0.96	3	120 (71.8%)
Particle-0.94	0	35 (21%)
Particle-0.92	0	4 (2.4%)
Particle-0.86	0	0 (0%)
Particle-0.76	0	0 (0%)

TABLE X
SEPARATION OF PARTICLES UNDER THE INLET VELOCITY OF 1 M/S

Inlet velocity: 1 m/s	Escaped at side outlet	Trapped at bottom outlet
Particle-0.96	36	131(78.4%)
Particle-0.94	3	164 (97.6%)
Particle-0.92	0	167 (100%)
Particle-0.86	0	104(62%)
Particle-0.76	0	0 (0%)

TABLE XI
SEPARATION OF PARTICLES UNDER THE INLET VELOCITY OF 1.6 M/S

Inlet velocity: 1.6 m/s	Escaped at side outlet	Trapped at bottom outlet
Particle-0.96	48	119 (71%)
Particle-0.94	17	150 (90%)
Particle-0.92	4	163 (97.6%)
Particle-0.86	0	167 (100%)
Particle-0.76	0	167 (100%)

TABLE XII
SEPARATION OF PARTICLES UNDER THE INLET VELOCITY OF 2.6 M/S

Inlet velocity: 2.6 m/s	Escaped at side outlet	Trapped at bottom outlet
Particle-0.96	55	112 (67%)
Particle-0.94	26	141 (84%)
Particle-0.92	1	166 (99.4%)
Particle-0.86	0	167 (100%)
Particle-0.76	0	167 (100%)

TABLE XIII
SEPARATION OF PARTICLES UNDER THE INLET VELOCITY OF 3.6 M/S

Inlet velocity: 3.6 m/s	Escaped at side outlet	Trapped at bottom outlet
Particle-0.96	49	118 (70.6%)
Particle-0.94	26	141 (84.4%)
Particle-0.92	15	152 (91%)
Particle-0.86	5	162 (97%)
Particle-0.76	0	167 (100%)

TABLE XIV
SEPARATION OF PARTICLES UNDER THE INLET VELOCITY OF 4.6 M/S

Inlet velocity: 4.6 m/s	Escaped at side outlet	Trapped at bottom outlet
Particle-0.96	55	112 (67%)
Particle-0.94	25	142 (85%)
Particle-0.92	17	150 (90%)
Particle-0.86	9	158 (94.6%)
Particle-0.76	0	167 (100%)

TABLE XV
SEPARATION OF PARTICLES UNDER THE INLET VELOCITY OF 5.6 M/S

Inlet velocity: 5.6 m/s	Escaped at side outlet	Trapped at bottom outlet
Particle-0.96	61	106 (63.5%)
Particle-0.94	28	139 (83%)
Particle-0.92	19	150 (90%)
Particle-0.86	11	156 (93.4%)
Particle-0.76	0	167 (100%)

TABLE XVI
SEPARATION OF PARTICLES UNDER THE INLET VELOCITY OF 6.6 M/S

Inlet velocity: 6.6 m/s	Escaped at side outlet	Trapped at bottom outlet
Particle-0.96	57	110 (66%)
Particle-0.94	34	133 (79.6%)
Particle-0.92	23	144 (86%)
Particle-0.86	14	153 (91.6%)
Particle-0.76	0	167 (100%)

TABLE XVII
SEPARATION OF PARTICLES UNDER THE INLET VELOCITY OF 7.6 M/S

Inlet velocity: 7.6 m/s	Escaped at side outlet	Trapped at bottom outlet
Particle-0.96	55	112 (67%)
Particle-0.94	20	145 (86.8%)
Particle-0.92	6	161 (96.4%)
Particle-0.86	1	166 (99.4%)
Particle-0.76	0	167 (100%)

TABLE XVIII
SEPARATION OF PARTICLES UNDER THE INLET VELOCITY OF 8.6 M/S

Inlet velocity: 8.6 m/s	Escaped at side outlet	Trapped at bottom outlet
Particle-0.96	49	118 (70.7%)
Particle-0.94	21	146 (87.4%)
Particle-0.92	15	152 (91%)
Particle-0.86	2	165 (98.8%)
Particle-0.76	0	167 (100%)

TABLE XIX
SEPARATION OF PARTICLES UNDER THE INLET VELOCITY OF 9.6 M/S

Inlet velocity: 9.6 m/s	Escaped at side outlet	Trapped at bottom outlet
Particle-0.96	52	115 (69%)
Particle-0.94	24	143 (85.6%)
Particle-0.92	14	153 (91.6%)
Particle-0.86	2	165 (98.8%)
Particle-0.76	0	167 (100%)

The separations of particles lighter than water with the feeding velocity of 1.6m/s and above are shown in Tables XI-XIX. Fig. 6 shows the variation of separation efficiency with increasing fending velocity for particles with various densities less than water. It seems that a feeding velocity beyond 1.6 m/s does not necessary increase the separation efficiency. Fig. 6 once again confirms that the density

difference between the particle and the medium liquid is a more prominent factor controlling the separation efficiency.

The relationship between the pressure drop and the feed flow velocity is shown in Fig. 7 which shows that the pressure drop rises with increasing in feed flow velocity (rate). As the simulation indicates that increase of the feed flow velocity beyond certain level does not contribute to the improvement of separation efficiency which also causes greater energy consumption, a lower feed velocity of around 1.6 m/s may provide a good balance between the efficiency and cost for this specific case.

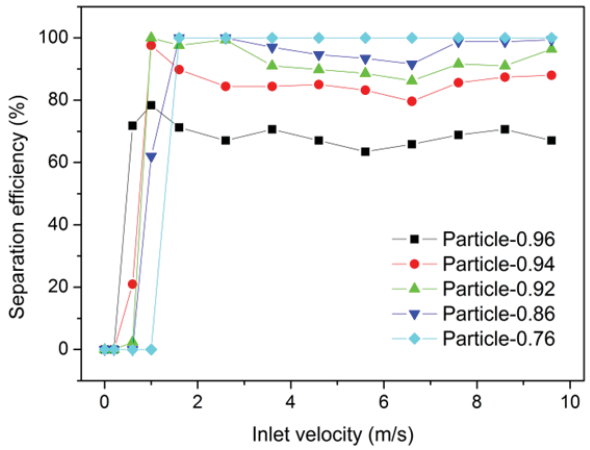

Fig. 6 Correlation of separation efficiency with inlet velocity

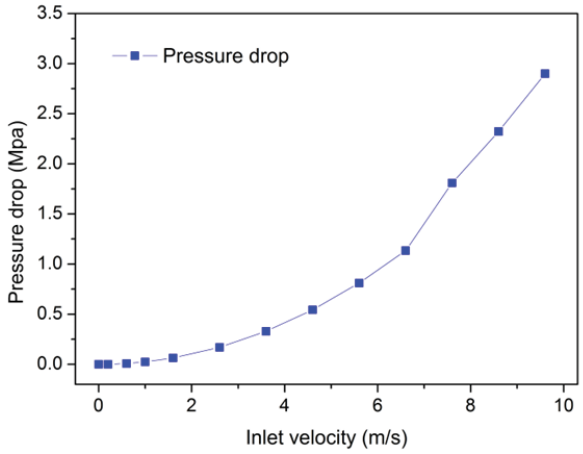

Fig. 7 Correlation of pressure drop with inlet velocity

V. Conclusions

In this study, the potential of a Vorsyl separator on the separation of plastic particles with different densities was numerically investigated. The factors influencing the separation performance were analyzed which includes the density difference between the particle and the liquid medium, the split ration, the feeding velocity and the pressure drop in the Vorsyl separator. The following results have been obtained:

- All particles that are heavier than water have larger centrifugal force which allows them to move along the wall of the Vorsyl chamber, reach the bottom and leave the separation through the side outlet. Whilst most portion of particles with density lower than liquid move to the center, enter the vortex finder and leave the separator through the bottom outlet. Therefore, particles collected at the bottom outlet are pure and clean.
- The separation efficiency is positively correlated with the density difference between medium liquid and the particle
- The separation efficiency of the Vorsyl separator can be improved by an increasing split ratio, especially for particles that have a small density difference to the medium liquid.
- The Vorsyl separator may not be workable when the feeding velocity is lower than a certain critical feeding velocity.
- An increasing feeding velocity results in increased pressure drop, however not necessarily increases the separation efficiency. An economic operation velocity balancing the efficiency and cost is therefore favorable.

References

[1] Wang, C.-q., et al., Flotation separation of waste plastics for recycling-A review. Waste Management, 2015. 41: p. 28-38.
[2] Yuan, H., et al., Study on the hydrocyclonic separation of waste plastics with different density. Waste Management, 2015. 45: p. 108-111.
[3] Fraunholcz, N., Separation of waste plastics by froth flotation - A review, part I. Minerals Engineering, 2004. 17(2): p. 261-268.
[4] Abbott, J., K.W. Bateman, and R.W. Shaw, Vorsyl separator, in Vorsyl separator, Proc. 9th Commonwealth Mining and Metall. Congr., London, Pap. 33, 1969, 1 - 19. 1969.
[5] Banerjee, P.K., et al., A plant comparison of the vorsyl separator and dense medium cyclone in the treatment of Indian coals. International Journal of Mineral Processing, 2003. 69(1–4): p. 101-114.
[6] ANSYS. ANSYS FLUENT 14.0 User's Guide. 2011 2012.03.01; Available from: http://148.204.81.206/Ansys/150/ANSYS%20Fluent%20Users%20Guide.pdf.
[7] Najafi, A.F., S.M. Mousavian, and K. Amini, Numerical investigations on swirl intensity decay rate for turbulent swirling flow in a fixed pipe. International Journal of Mechanical Sciences, 2011. 53(10): p. 801-811.
[8] Fokeer, S., I.S. Lowndes, and D.M. Hargreaves, Numerical modelling of swirl flow induced by a three-lobed helical pipe. Chemical Engineering and Processing: Process Intensification, 2010. 49(5): p. 536-546.
[9] Speziale, C.G., S. Sarkar, and T. B. Gatski, Modelling the Pressure-Strain Correlation of Turbulence: An Invariant Dynamical Systems Approach. J. Fluid Mech, 1991. 227: p. 245-272.